DOI: 10.13009/EUCASS2017-646

Prediction of the residual thrust of 2nd and 3rd Vega Launcher Solid Rocket Motors stages after the burn-out, due to internal thermal protection pyrolysis

D. Schiariti, F. Paglia**, E. Gizzi***, C. Milana****, D. Barbagallo*****, A. Neri*******
**AVIO S.p.A., via Ariana km 5.2-Colleferro (Rome), Italy 00034*
daniele.schiariti@avio.com
*** AVIO S.p.A., via Ariana km 5.2-Colleferro (Rome), Italy 00034*
fabio.paglia@avio.com
****AVIO S.p.A., via Ariana km 5.2-Colleferro (Rome), Italy 00034*
emanuela.gizzi@avio.com
*****ELV S.p.A., Via degli Esplosivi 1-Colleferro (rome), Italy, 00034*
claudio.milana@elv.it
******ESA/ESRIN, Via Galileo Galilei 64-Frascati (Rome), Italy 00044*
daniele.barbagallo@esa.int
*******ESA/ESRIN, Via Galileo Galilei 64-Frascati (Rome), Italy 00044*
agostino.neri@esa.int

Abstract

Vega ESA's satellite multi-stage launch vehicle has a configuration foreseeing three solid propellant stages and a fourth liquid stage. The Vega Solid Rocket Motors contain an aluminized propellant and an ablative internal thermal protection; after motor burn-out, the internal thermal protection has a porous char at elevated temperature and a pyrolysis zone still decomposing, that drives a thermal wave inside to the material, becoming a source of heat for the production of gases due to the pyrolysis of the residual virgin material. The pyrolytic action creates a residual thrust, which in the case of orbital transfer motor can affect the subsequent staging and so must be predicted. The object of this study has been to develop a technique for predicting the amount and the duration of the described residual thrust. The thermal degradation model of the internal thermal protection of the Solid Rocket Motors supplies the mass flow rate of the pyrolysis gas and its temperature as a function of time and, together with motor configuration (nozzle throat diameter), allow the estimation of the chamber pressure, of the thrust and of the induced impulse by internal thermal protection material pyrolysis phenomena. Comparison between the predicted values of thrust and the experimental data acquired during Vega flights, from mission VV01 to mission VV08, has been performed, showing very good agreement between numerical results obtained by the model and the experimental measures.

1. Introduction

Vega is the ESA's satellite multi-stage launch vehicle, designed to send small satellites into Low Earth Orbit (LEO). Vega Launcher configuration foresees three solid propellant stages (1st P80, 2nd Zefiro 23 and 3rd Zefiro 9) and a fourth liquid stage (Avum), see Figure 1. The Vega Solid Rocket Motors contain an aluminized propellant and an ablative internal thermal protection, necessary to protect the composite case during the motor operative life; during the firing, the thermal degradation mechanism of the internal thermal protection can be explained with Figure 2: as the insulating material is heated by the gas at elevated temperature inside the combustion chamber, the original virgin material pyrolyzes and yields a pyrolysis gas, which percolates away from the pyrolysis zone and the porous residue, consisting of a carbonaceous char. This is the degradation mechanism occurring during the firing. Since the end of firing, the thermal terms due to the free stream don't act on the internal thermal protection surface, but the porous

DOI: 10.13009/EUCASS2017-646

char at elevated temperature and a pyrolysis zone still decomposing are present, driving a thermal wave from the surface to the core of the material, still virgin at the end of firing. The diffusion of the thermal wave inside of the material, due to the strong thermal gradient inside the thickness of thermal protection, increases the temperature inside the residual pyrolysis and virgin zones, allowing to the internal thermal protection material to keep on degrade and generate pyrolysis gas that, from decomposing zone, flows inside the motor and out from the combustion chamber, through the nozzle. The mass flow of pyrolysis gas creates a residual thrust, which, in the case of orbital transfer motors as Zefiro 23 and Zefiro 9 for Vega Launcher, can affect the mission design and so must be predicted. Dedicated analyses have been performed for the 2nd and 3rd Vega Launcher stages Solid Rocket Motors, in order to evaluate the decomposition of the thermal protection after the firing and to give an estimation of the mass of the thermal protection lost for the thermal wave conduction from the charred surface to the core of the material. The internal thermal protection behaviour, in terms of insulating performance and degradation phenomena, has been simulated with CMA92 code, on the basis of models developed and validated in the frame of Vega static firing tests and flights. The thermal-degradation analyses have been performed from the motors ignition up to 200 seconds after the end of the firing (so simulating the firing and after firing effects on the thermal protection), allowing to calculate the mass flow rate of the pyrolysis gas as a function of time, together with its temperature evolution. On the basis of pyrolysis gas mass flow rate, its temperature and throat diameter, the chamber pressure has been calculated, allowing the estimation of the thrust and impulse induced by the pyrolysis phenomena both on Zefiro 23 and Zefiro 9 Solid Rocket Motors. The results obtained by the numerical model built to predict the residual thrust after bun out of Orbital Transfer Motors due to the pyrolysis gas are compared with experimental data acquired in the frame of Vega Launcher flights, from mission VV01 to mission VV08, allowing to verify its consistency with experimental data and its suitability to work as predicting tool.

2.Numerical Model description

2.1 CMA92 code

The CMA92 code is an implicit, finite-difference computational procedure for computing the one-dimensional transient transport of thermal energy in a three-dimensional isotropic material, which can ablate from a front surface and which can decompose in-depth.
The code has the capability of performing computations with general convection-radiation surface boundary conditions, coupled with thermochemical erosion, to model chamber conditions during the motor burn. An additional option exists which allows the specification of a radiation view factor and an incident radiation flux as a function of time, to simulate the transient cool down and insulation decomposition subsequent to motor burnout.
The in-depth solution procedure is a transient heat conduction calculation which is coupled to a pyrolysis rate calculation. Since many decomposing char-forming materials appear to behave as three independently pyrolyzing components, the program uses a three-component decomposition model, so the instantaneous density of decomposing material is given by equation **(1):**

$$\rho = \Gamma(\rho_A + \rho_B) + (1 - \Gamma)\rho_c \quad \textbf{(1)}$$

where A and B represent components of the matrix, C represents the reinforcing material and Γ is the volume fraction of matrix. Each of the three components can decompose following the relation coming from the Arrhenius law (equation **(2)**):

$$\frac{\partial \rho_i}{\partial t}\Big)_y = -B_i exp\left(-\frac{E_{a_i}}{RT}\right)\rho_{0_i}\left(\frac{\rho_i - \rho_{r_i}}{\rho_{0_i}}\right)^{\Psi_i} \quad \textbf{(2)}$$

where ρ_{ri} is the residual or terminal density of component *i*, ρ_{0i} is the original density of component *i*, B_i is the pre-exponential factor of component *i*, E_{ai} is the activation energy of the component *i*, R is the universal gas constant and Ψ_i is the decomposition reaction order of the component *i*. The decomposing behaviour of Zefiro 23 and Zefiro 9 internal thermal protection material, experimentally characterized by means of TGA (thermogravimetric analysis) performed at different heating rates (an example is reported in Figure 4), confirms its conformity with the modellization described before (three decomposing materials with separated Arrhenius parameters).
For the purpose of writing the in-depth energy balance differential equation, the x-coordinate system is introduced, tied to the receding surface, as shown in Figure 3. In this system, the energy equation assumes the following form:

DOI: 10.13009/EUCASS2017-646

$$\rho c_p \frac{\partial T}{\partial t}\Big)_x = \frac{1}{A}\frac{\partial}{\partial x}\Big(kA\frac{\partial T}{\partial x}\Big)_t + \big(h_g - \bar{h}\big)\frac{\partial \rho}{\partial t}\Big)_y + \dot{s}\rho c_p \frac{\partial T}{\partial x}\Big)_t + \frac{\dot{m}_g}{A}\frac{\partial h_g}{\partial x}\Big)_t \quad \textbf{(3)}$$

in which the individual terms have physical meaning which may be interpreted as follows (from left to right in **(3)**): rate of energy storage of sensible energy, net rate of thermal conduction, pyrolysis energy rate, convection rate of sensible energy due to coordinate system movement, and net rate of energy convected with pyrolysis gas passing a point.

As in all finite difference procedures, each step of the solution is made over an incremental time step of Δt. Each computational step has three main events: internal decomposition, internal energy balance and surface boundary energy balance. Computation of three events give new values of nodal densities, pyrolysis gas flow, nodal temperatures, surface temperature and ablation rate. The program is then ready for the next step.

The pyrolysis event is computed for each node in the main material by means of Arrhenius law, summed over the three components. The nodal $\partial\rho/\partial t$ gives the contribution to pyrolysis mass flow rate. Note that the old known nodal temperatures are used in the pyrolysis calculations. The internal energy balance equation then is calculated implicitly for each node, using new temperatures in the heat conduction terms. The energy balance is linked explicitly to the decomposition events, since the pyrolysis gas fluxes used in the energy balance are derived from the explicit decomposition calculation. The energy balance is also linked explicitly to the surface boundary condition through the use of an old recession rate in all convection terms involving fluxes of solids. All other links to the surface events are implicit.

In addition to the Arrhenius decomposition parameters, the CMA92 program requires several other material property inputs. These include specific heat, thermal conductivity and emissivity for both the virgin and charred states as functions of temperature. These properties have been obtained by dedicated experimental activities performed in the frame of Vega Launcher development, when the internal thermal protection material has been fully characterized and the developed models have been qualified by means of bench firing tests and flight measurements and evidences.

2.2 Model description

Dedicated analyses have been performed for Zefiro 9 and Zefiro 23 Solid Rocket Motors, in order to evaluate the decomposition of the thermal protection after the end of firing and to give an estimation of the mass of thermal protection lost for the thermal wave conduction from charred surface to the core of the material.

In accordance to the methodology developed in the frame of Vega program to estimate the mass ejected during the firing, the volume of internal thermal protection has been discretized in several control points (as described in §2.1, CMA92 code is mono-dimensional), where the charred, the pyrolysis and the virgin residual thicknesses have been calculated with CMA92 code, together with the temperature field inside the material along the motor, with the models validated in the frame of Vega bench firing tests and flights. At the end of the motor firing, inside the thermal protection is present a strong thermal gradient between the surface, charred, and the residual virgin thickness, so the heat conduction is a phenomenon that keeps on act for the period following the burn-out, with all the linked phenomena (i.e. thermal degradation of the material): more elevated is the energy “stored” inside the chamber and decomposing thickness, more elevated is the heat flux that, for conduction, is driven inside the residual virgin thickness and can induce the further thermal degradation of material for pyrolysis phenomena.

The thermal-degradation analyses have been performed from the motor ignition up to 200 seconds after the end of firing (so simulating the firing and after firing effects on the thermal protection), on the different zones of the Solid Rocket Motors, taking into account both thermal protection material and composite case, allowing to calculate the mass flow rate of the pyrolysis gas as a function of time, together with its temperature evolution. The simulation of the firing phase has been performed using the qualified thermal degradation models and applying the validated convective and radiative boundary conditions and materials properties (supplying erosion, degraded and virgin thicknesses, temperature trends inside the thickness consistent with experimental data experienced with bench firing tests and Vega flights); the post firing phase has been simulated as a cool down phase (see §1.2), applying the radiative heat fluxes due to the elevated temperature inside the chamber.

DOI: 10.13009/EUCASS2017-646

The results reported in the paper are focused on the after firing phases: on the basis of pyrolysis gas mass flow rate, its temperature and nozzle throat diameter, the chamber pressure is calculated using the basic standard equations, allowing the calculation of the thrust and of the impulse induced by the pyrolysis phenomena.

3.Analyses results

3.1 Zefiro 9

In accordance to the methodology developed in the frame of Vega program to estimate the mass ejected during the firing of Zefiro 9 Solid Rocket Motor, the volume has been discretized in several control points where the charred, the pyrolysis and the virgin residual thicknesses have been calculated with CMA92 code, together with the temperature field inside the material along the motor, with the models validated in the frame of Vega bench firing tests and flights. As reference, the results of calculation in correspondence of the aft part of cylindrical part of Zefiro 9, starting from the end of firing up to 200 seconds, is reported in Figure 5, where:

- Twall is the temperature of the charred surface;
- TC1 is a thermocouple inside the charred thickness;
- TC2 is a thermocouple in the pyrolysis thickness;
- TC3, TC4, TC5 and TC6 are thermocouples inside the virgin residual material at the end of firing;

As can be seen, the diffusion of thermal wave from the external surface toward the virgin thickness induces the cooling of the charred material, but a strong heating of the virgin residual thickness of thermal protection, up to temperature when the degradation of the rubber occurs.
The simulation performed for the entire Zefiro 9 Solid Rocket Motor supplies the pyrolysis gas mass flow rate after the motor burn-out shown in Figure 6. The following considerations can be performed:

- In the first instants, the expelled mass is more elevated: this is due to the fact that this phase is still strongly influenced by firing: in particular, in correspondence of the domes, zones with elevated exposure times to hot gas, the pyrolysis thickness (already in decomposing phase at burn-out) is elevated, so the decomposition phenomenon, already acting during the motor firing, keeps on occurring in the following instants.
- After few seconds, the thermal wave diffusion inside of the material induces the degradation of material in virgin state at the end of firing, in particular on the cylindrical part, where the installed thicknesses are lower with respect to the domes;

The temperature of the pyrolysis gas has been calculated as a function of time with a thermal balance between the charred porous thickness and the pyrolysis gas coming from the degradation zone; the result is shown as a function of time in Figure 7.
The re-built trend of chamber pressure due to the pyrolysis gas is shown in Figure 8. On the basis of the pyrolysis gas mass flow rate, its temperature and chamber pressure, the residual thrust due to the internal thermal protection degradation after the Zefiro 9 Solid Rocket Motor burn-out has been calculated and the result is shown in Figure 9.
In Figure 10 the following curves are reported:

- Nominal thrust evaluated by ballistic model;
- Average value of Zefiro 9 thrust rebuilt by VV01-VV08 missions data;

It is worth to note that reported data show a very good correlation of the nominal thrust with respect to the average value of the flight re-built thrust.

3.2 Zefiro 23

In accordance to the methodology developed in the frame of Vega program to estimate the mass ejected during the firing of Zefiro 23 Solid Rocket Motor, the volume has been discretized in several control points, where the charred, the pyrolysis and the virgin residual thicknesses have been calculated with CMA92 code, together with the temperature field inside the material along the motor, with the models validated in the frame of Vega bench firing tests and flights.
The simulation has been performed for the entire Z23 motor, obtaining the mass flow rate of pyrolysis gas after burn-out shown in Figure 11. The calculation of pyrolysis gas temperature, chamber pressure and residual thrust after burn-out have been performed with the same methodology adopted for the Zefiro 9 analysis, so the hypotheses described in §3.1 are fully applicable. The calculated Zefiro 23 mass flow rate temperature and thrust are shown in Figure 12 and Figure 13.
In Figure 14 the following curves are reported:

- Thrust evaluated by mathematical model;

DOI: 10.13009/EUCASS2017-646

- Average value of Zefiro 23 thrust re-built by VV01—VV08 missions data;

As for Zefiro 9, the data reported in Figure 14 show a very good correlation of the nominal numerical thrust with respect to the average value of the flight re-built thrust.

4.Conclusion

A technique has been developed for predicting the post burn residual thrust in a Solid Rocket Motor due to the pyrolysis of internal thermal protection, occurring not only during the firing, but also after the burn-out, due to the severe environment inside the motor. The developed methodology has been applied to the second and third stages of Vega ESA's satellite multi-stage launcher, Zefiro 23 and Zefiro 9 Solid Rocket Motors: the thermal-degradation analyses have been performed from the motors ignition up to 200 seconds after the end of firing (so simulating the firing and after-firing effects on the internal thermal protection), allowing to calculate the mass flow rate of pyrolysis gas as a function of time, together with its temperature evolution. On the basis of pyrolysis gas mass flow rate, its temperature and nozzle throat diameter, the chamber pressure has been calculated, allowing the estimation of the thrust and impulse induced by the pyrolysis phenomena both on Zefiro 23 and Zefiro 9 Solid Rocket Motors. The obtained results have been compared with the available data coming from measurements performed during Vega flights from mission VV01 to mission VV08, showing very good agreement between numerical results obtained by models and the experimental measures. The correlated model is a suitable tool for the prediction of the residual thrust and impulse after a Solid Rocket Motor burn-out, allowing at system level to consolidate the mission design.

5. Figures and tables

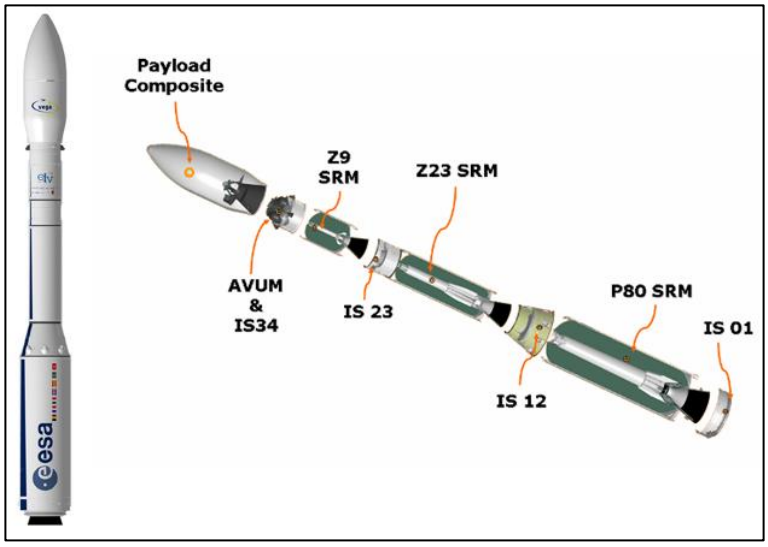

Figure 1: VEGA launcher configuration

DOI: 10.13009/EUCASS2017-646

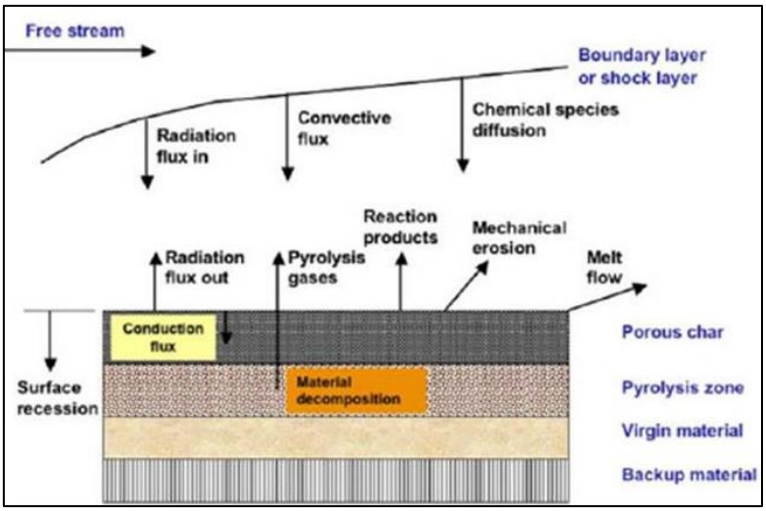

Figure 2: Thermal degradation mechanism

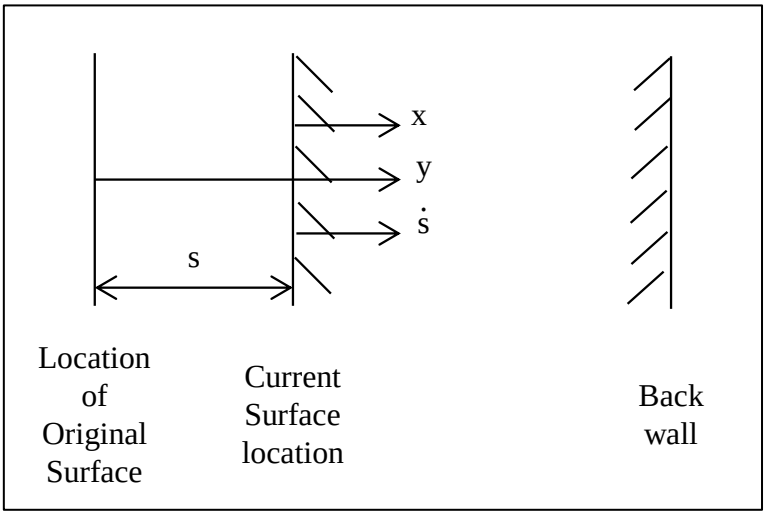

Figure 3: CMA92 coordinate system

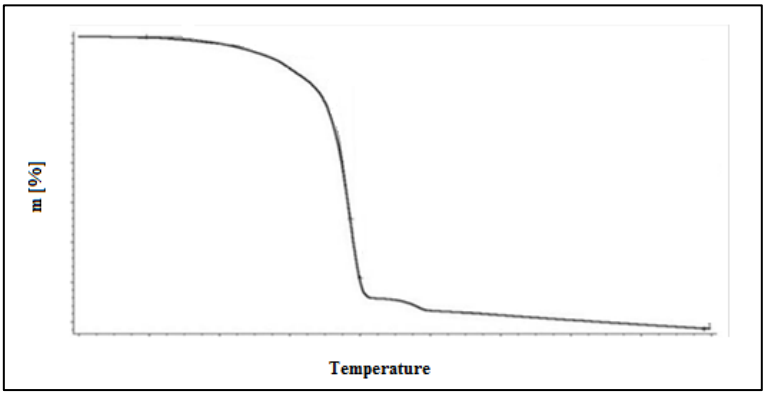

Figure 4: Zefiro 23 and Zefiro 9 internal thermal protection TGA

DOI: 10.13009/EUCASS2017-646

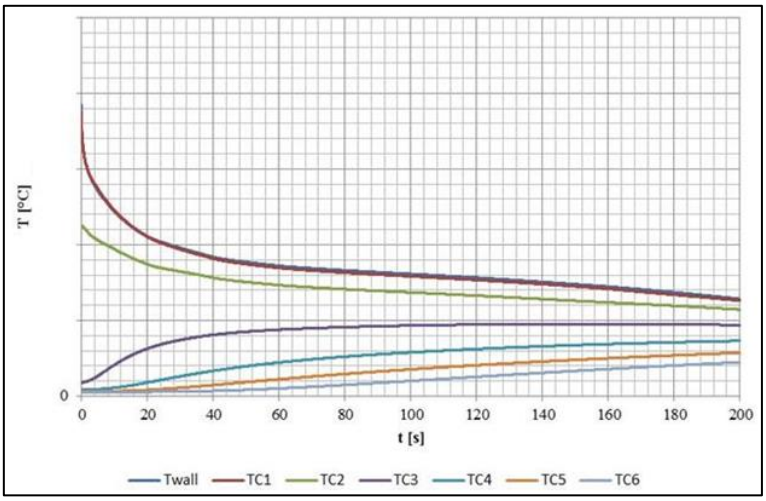

Figure 5: Zefiro 9 temperatures inside internal thermal protection after motor burn-out

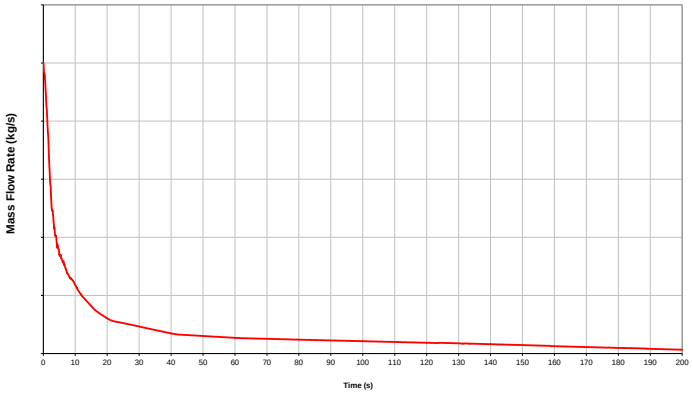

Figure 6: Zefiro 9 pyrolysis gas mass flow rate during motor burn-out

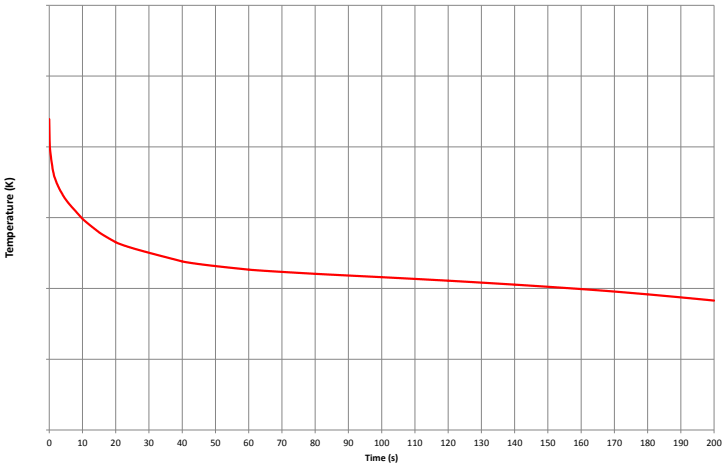

Figure 7: Zefiro 9 pyrolysis gas temperature during motor burn-out

DOI: 10.13009/EUCASS2017-646

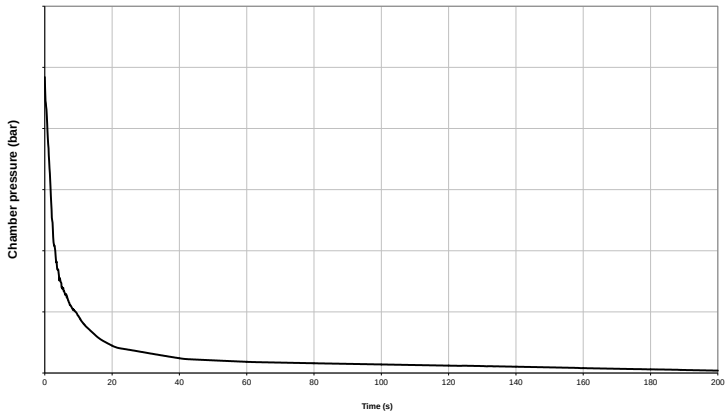

Figure 8: Zefiro 9 chamber pressure during motor burn-out

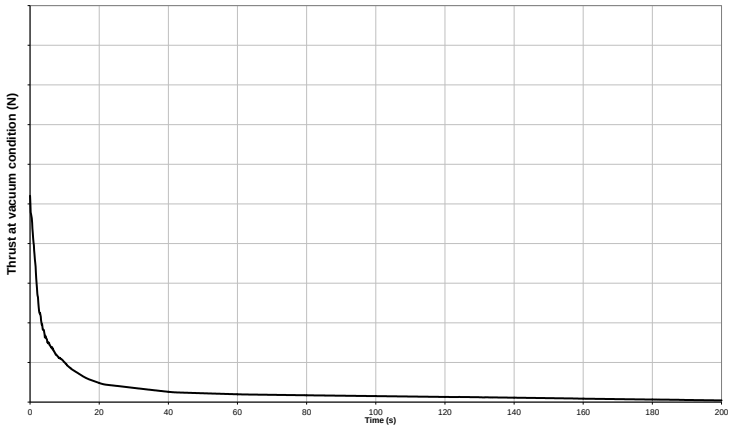

Figure 9: Zefiro 9 Pyrolysis thrust estimation in vacuum during motor burn-out

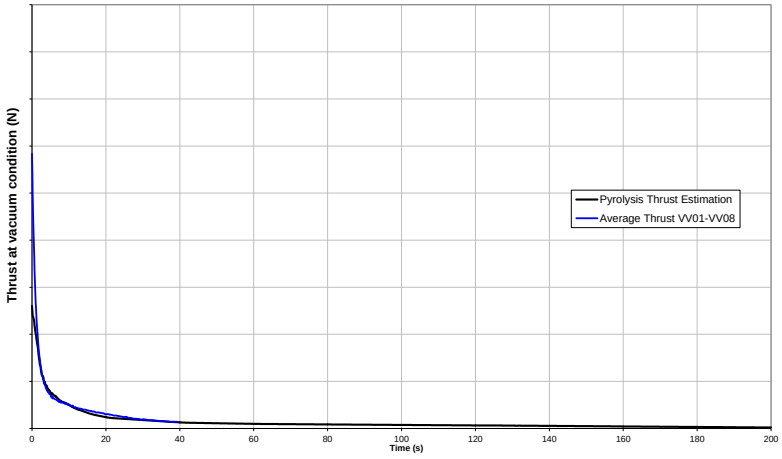

Figure 10: Zefiro 9 Pyrolysis vacuum thrust estimation vs experimental data during motor burn-out

DOI: 10.13009/EUCASS2017-646

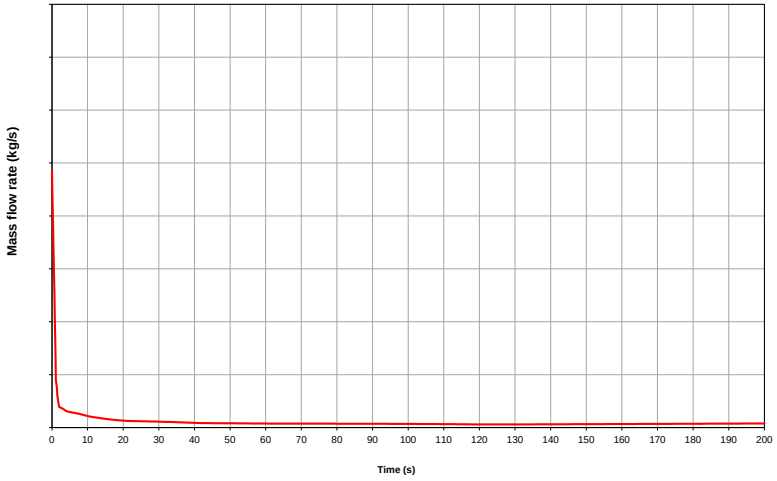

Figure 11: Zefiro 23 pyrolysis gas mass flow rate during motor burn-out

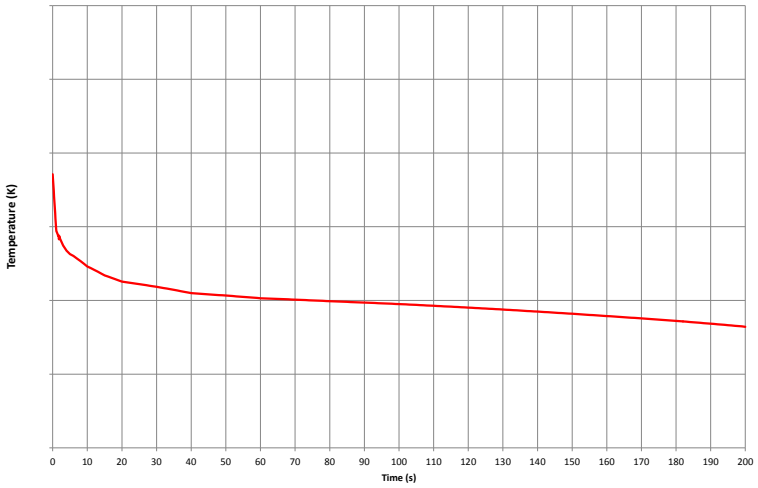

Figure 12: Zefiro 23 pyrolysis gas temperature during motor burn-out

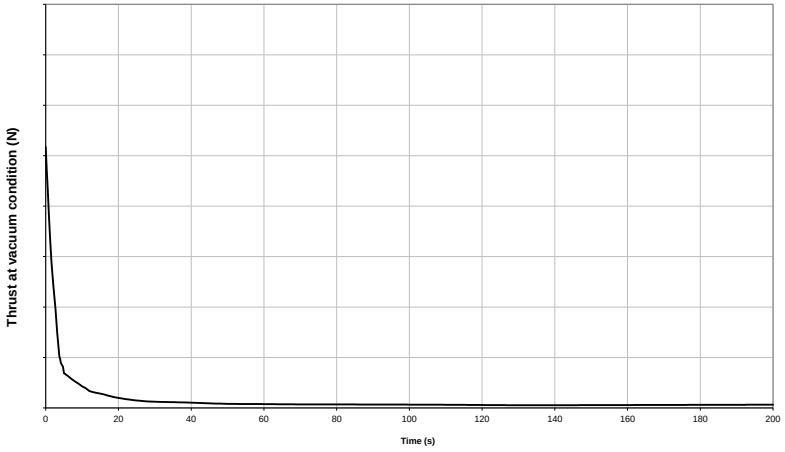

Figure 13: Zefiro 23 pyrolysis thrust estimation in vacuum during motor burn-out

DOI: 10.13009/EUCASS2017-646

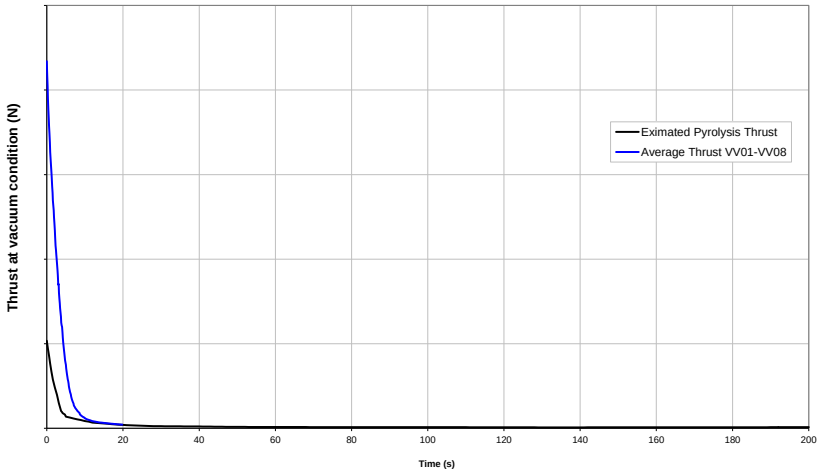

Figure 14: Zefiro 23 Pyrolysis vacuum thrust estimation vs experimental data during motor burn-out

References

[1] C. B. Moyer, R. A. Rindal. 1968. Finite Difference Solution for the In-Depth Response of Charring Materials Considering Surface Chemical and Energy Balances. In: An analysis of the coupled chemically reacting boundary layer and charring ablator, Part II.